



Effect of electrochemical state on corrosion–wear behaviors of TC4 alloy in artificial seawater

Jun CHEN^{1,2,3}, Qing ZHANG^{1,3}

1. School of Materials Science and Engineering,

Henan University of Science and Technology, Luoyang 471023, China;

2. State Key Laboratory of Solid Lubrication, Lanzhou Institute of Chemical Physics,
Chinese Academy of Sciences, Lanzhou 730000, China;

3. Collaborative Innovation Center of Nonferrous Metals of Henan Province, Luoyang 471023, China

Received 6 April 2015; accepted 14 September 2015

Abstract: The electrochemical and corrosion–wear behaviors of TC4 alloy in artificial seawater were studied. And the influences of electrochemical state on passive behavior, failure mechanism of passive film and corrosion–wear synergy were emphatically analyzed. The corrosion–wear analysis of the alloy was fulfilled by methods of mass loss, electrochemical testing and scanning electron microscope (SEM). It can be observed that the cathodic shift of open circuit potential and three order of magnitude increase of current density can be obtained during corrosion–wear process. Total corrosion–wear loss increases with increasing applied potential, confirming the synergy between wear and corrosion. High polarisation potential results in low coefficient of friction and high corrosion rate. The relative contribution of pure mechanical wear to total material loss decreases obviously with the increase of potential from open circuit potential to 0.9 V during corrosion–wear. Contributions of wear-induced-corrosion and corrosion-induced-wear are significant especially at higher potentials.

Key words: TC4 alloy; corrosion–wear; electrochemical state; synergistic effect

1 Introduction

Titanium-based alloys are the most popular corrosion-resistant metallic materials used in aerospace, marine, automotive and biomedical industries due to its excellent corrosion resistance, high strength and good fatigue. The excellent corrosion resistance of titanium alloys is attributed to the formation of stable, continuous and protective oxide film on the metal surface in contact with corrosive environment. However, the natural passive film is poor and thin with a thickness of 3–5 μm . Despite its high corrosion resistance in many corrosive conditions, the natural oxide film exhibits poor corrosion–wear properties [1–5].

Protective passive films usually form on the surface of many alloys in corrosive environments, which can make the alloy maintaining passivity and prevent dissolution of bare metal. However, the protective passive film is not stable especially subjecting to

combined corrosion and wear attack in many situations. These will cause destruction removal of passive film from contact surface, leading to accelerated metal dissolution, which in turn can result in accelerated wear [6–10]. Material loss caused by corrosion wear is usually much greater than the simple sum of pure wear and corrosion. So, corrosion-induced-wear and wear-induced-corrosion will be the dominant factor of material failure [11,12]. Over the past few years, study on corrosion wear of alloys is a research hot spot. Efforts have been made to identify the corrosion wear behaviors of passive metals, especially focusing on the synergistic effect between corrosion and wear [13,14]. HENRY et al [15,16] have studied the corrosion wear behaviors of 316L stainless steel and Ti6Al4V titanium alloy sliding against an alumina ball in 0.5 mol/L H_2SO_4 solution under different applied electrochemical potentials (cathodic, free or anodic potential) and found that wear rate of Ti6Al4V alloy is much higher than that measured for 316L stainless steel and nickel alloy. Moreover, the

wear loss for the three alloys under anodic condition is much higher than that under cathodic and free potential conditions, conforming that electrochemical state has a significant effect on the corrosion–wear behaviors. SERRE et al [5] and BARRIL et al [17] have studied the electrochemical effects on the fretting corrosion behaviors of Ti6Al4V in 0.9% sodium chloride solution. It can be obtained that wear rate of Ti6Al4V alloy depends critically on the prevailing electrode potential. At anodic potentials, the oxidation of third body particles dramatically decreases the mechanical energy required for wear. PRIYA et al [18] have studied the wear and tribocorrosion behaviors of 304LSS, Zr-702, zircaloy-4 and Ti-grade2 and the synergy between wear and corrosion for all alloys led to degradation of the passive materials in tribocorrosion condition. However, the fundamental mechanism that determines the wear–corrosion synergism during corrosion wear of Ti-based alloy with different electrochemical states in chloride containing solution has not been fully understood.

The purpose of the present research is to assess the effect of electrochemical state on corrosion wear behaviors of TC4 titanium alloy in artificial seawater and the synergistic effect between corrosion and wear is quantitatively evaluated. Corrosion wear experiments are completed in a developed apparatus allowing for well-controlled mechanical and electrochemical conditions.

2 Experimental

The researched metallic material in this experiment was TC4 titanium-based alloy with the following chemical composition: 6.25% Al, 4.21% V, 0.22% C, 0.19% Fe, balance Ti. For the corrosion–wear tests, the TC4 alloy was machined into specimens of a ring (outer diameter: 54 mm, inner diameter: 38 mm). Only the upper surface of the metallic specimen was in touch with corrosive liquid and other surfaces are covered with paint to avoid electrochemical confusion. Working area of TC4 specimen was 11.5 cm². The selected counterpart was Al₂O₃ pin for insulation with a flat surface at one end of a cylinder (diameter: 4.7 mm, height: 13 mm). Before each corrosion–wear experiment, all specimens were polished down to mirror quality using 220, 500, 1000 grade grit papers and with 1 μm diamond suspension, following by cleaning in acetone. Corrosive electrolyte was artificial seawater prepared according to ASTM D1141–98 standard. The pH value of this solution was 8.2. All corrosion wear tests were carried out at room temperature (20–25 °C).

Corrosion wear setup combined with in-situ electrochemical measurements is illustrated in Fig. 1.

Sliding wear tests were completed using a MMW–1 pin-on-disk tribometer. The stationary ring was abraded by a rotating pin during sliding. Normal load was applied through a lever mechanism and friction coefficient can be measured through an attached strain gauge and recorded by computer acquisition system. In-situ electrochemical measurements during sliding can be performed using a CHI760C potentiostat. For electrochemical experiment, TC4 specimen was used as working electrode (WE). A saturated calomel electrode (SCE) close to the TC4 specimen surface serves as the reference electrode (RE) and platinum wire was acted as counter electrode (CE). All potentials in this work were given with respect to the saturated calomel electrode (SCE). Electrolytic cell was filled with about 300 mL corrosive liquid. Rotation speed in this experiment was 200 r/min and normal load maintains at 100 N. The corrosion wear time was 60 min. During corrosion wear test, wear track was a ring with a mean diameter of 46 mm and a width of 4.7 mm (diameter of Al₂O₃ pin). And area of wear track was 6.8 cm². After corrosion wear experiment, the TC4 specimen was ultrasonically cleaned in acetone. Gravimetric measurements before and after experiment were finished using analytical balance. Wear loss can be obtained as below:

$$V = \frac{m_0 - m_1}{\rho} \quad (1)$$

where V is the wear loss, m_0 is the mass of the alloy before corrosion wear, m_1 is the mass of the alloy after corrosion wear, and ρ is the density of the alloy. Morphologies of worn surfaces can be examined using JEM–5600LV scanning electron microscope (SEM).

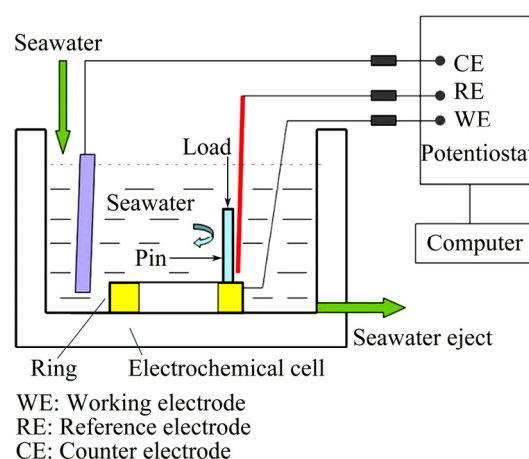


Fig. 1 Schematic diagram of corrosion wear apparatus

Several series of electrochemical experiments were conducted to assess the corrosion wear behaviors of TC4 alloy under different states: 1) Corrosion wear tests were completed under open circuit potential (OCP) condition and evolution of open circuit potential can be recorded;

2) Potentiodynamic measurements, involving measurement of polarization curves during corrosion wear and corrosion-only, were initiated after a stable open potential condition, which is performed at a sweep rate of 1.67 mV/s; 3) For obtaining different electrochemical states of TC4 alloy, potentiostatic tests during sliding were conducted at constant applied potentials and the current transients were measured.

3 Results and discussion

3.1 Electrochemical behaviors

Evolution of open circuit potential of TC4 alloy under corrosion–wear condition is shown in Fig. 2. It can be obtained that OCP drops sharply down to more negative value at the start of sliding. The cathodic shift phenomenon of OCP during corrosion–wear has been frequently observed for many passive metallic materials under similar experimental systems [19–21]. The drop of OCP can be expounded through the destruction of passive film formed in original surface by mechanical wear [22,23]. So, a galvanic coupling between passive surface and passive-damaged surface is formed. The damage of passive film may increase anodic reactions and cathodically polarize the surrounding surface, resulting in the cathodic shift of OCP. When friction stops, OCP starts to increase (anodic shift) abruptly. This indicates the re-establishment of passive state in wear track.

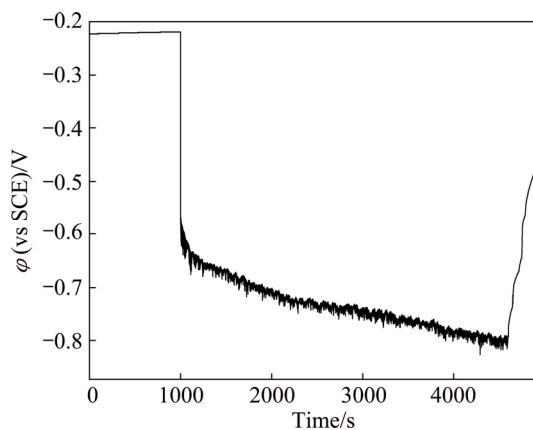


Fig. 2 Evolution of OCP (ϕ) as function of time for TC4 alloy under corrosion–wear condition

The appraisal of corrosion kinetics can be carried out by potentiodynamic polarization [22]. Polarization curves under corrosion-only and corrosion–wear conditions for TC4 alloy are shown in Fig. 3. Obviously, passive region can be seen for TC4 alloy and the passive current is very low, which suggests that the passivation ability of TC4 alloy is strong [19–21]. Polarization curve during corrosion–wear can analyze corrosion behaviors and repassivating ability when passive film is

mechanically damaged. Polarization curve during corrosion–wear exhibits significant current oscillations. It can be attributed to instability of experimental system and simultaneous process of destruction and recovery of passive film. In addition, friction couples contact positions of this experimental device change continuously, which contributes to oscillations of polarization curves also [24]. Corrosion potential during corrosion–wear is shifted to lower, more active potentials by about 0.3 V compared with corrosion-only curve, which is consistent with the outcome of OCP test. More importantly, corrosion current density during corrosion–wear is increased by three orders of magnitude compared with that under corrosion-only condition. Corrosion rate is significantly increased by sliding for TC4 alloy.

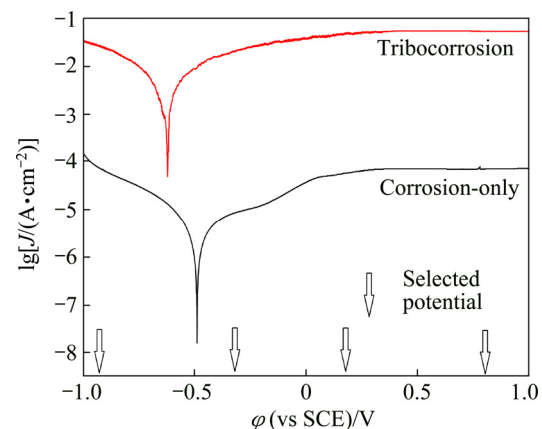


Fig. 3 Polarization curves under corrosion-only and tribocorrosion conditions

Another phenomenon obtained during corrosion–wear is the correlation between coefficient of friction (COF) and current density, as shown in Fig. 4, where the polarisation and COF measurements are synchronously fulfilled. During the potential sweep starting at the vicinity of -1 V, COF value is around 0.24 in the cathodic region. With the increase of potential from -1 V to corrosion potential, a slight decrease in COF can be marked. When the potential exceeds -0.2 V, a stable COF about 0.18 can be obtained. These results suggest that the destroy–repair of oxide film at anode potential helps to reduce COF. Anode polarisation results in low COF and high corrosion rate for TC4 alloy during corrosion–wear.

For potentiostatic experiments, a potential is applied to the metallic specimen using a three-electrode testing system. The selected potential is maintained at a fixed value during corrosion–wear test. Current and COF can be recorded continuously as a function of time to follow the evolution of corrosion kinetics and friction behaviors, respectively. A wide range of potentials are selected in

this work, as indicated by arrowed dotted lines marked in Fig. 3. For the purpose of assessing contribution of pure mechanical wear to total material loss, a sliding test is conducted at a cathodic potential of -0.9 V, which is determined at 0.2 V below the corrosion potential during corrosion–wear. Clearly, the measured current is cathodic before, during and after sliding test, confirming no corrosion as shown in Fig. 5. Under such a cathodic condition, TC4 alloy exhibits no corrosion. Similar procedures have been employed to evaluate mechanical wear component during corrosion–wear process [19–21].

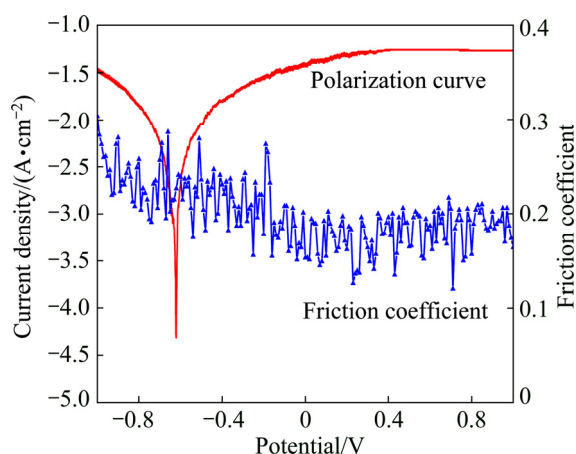


Fig. 4 Polarization curves and COF measured under corrosion–wear condition

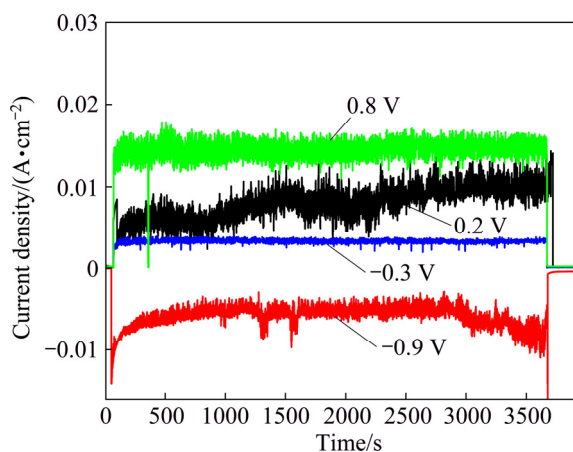


Fig. 5 Evolution of current density for TC4 alloy at different applied potentials

With the confirmation of pure mechanical contribution, it is imperative to determine the contribution of corrosion–wear synergism. Figure 5 shows the current transients measured at selected potentials of -0.3 , 0.2 and 0.8 V. It can be seen that corrosion current increases sharply at the beginning of sliding. Mechanical wear leads to thinning or local removal of passive film and results in sharp increase of anodic current. The cyclic abrasion maintains the current at relatively high value. When sliding stops, the current

decreases to a lower value quickly. Importantly, corrosion current increases obviously with the increase of applied potential, confirming significant wear–accelerated–corrosion phenomenon especially at anode potential during corrosion–wear.

3.2 Wear behavior

Figure 6 shows wear loss for TC4 alloy at OCP and applied potential conditions. It is evident that total wear loss significantly increases with increasing applied potential. At the cathodic potential (-0.9 V), the dissolution of the metal by corrosion is negligible, and material degradation proceeds mainly through mechanical wear, which results in low material loss. In anodic polarization and OCP conditions, material loss can be enhanced by corrosive attack, and synergistic effect between wear and corrosion results in high material loss. Clearly, corrosion has a significant effect on the material loss of TC4 alloy. Furthermore, the degradation of Al_2O_3 counterpart is negligible through volume loss analysis under all experimental conditions. Figure 7 illustrates the evolution of COF with time for TC4 alloy. All COF values reach a steady state exhibiting significant peaks at fairly regular time intervals. Such fluctuations are attributed to the formation and ejection of wear debris [25]. There is a general trend that COF decreases with increasing potential, although the COF values measured at OCP and -0.9 V are similar.

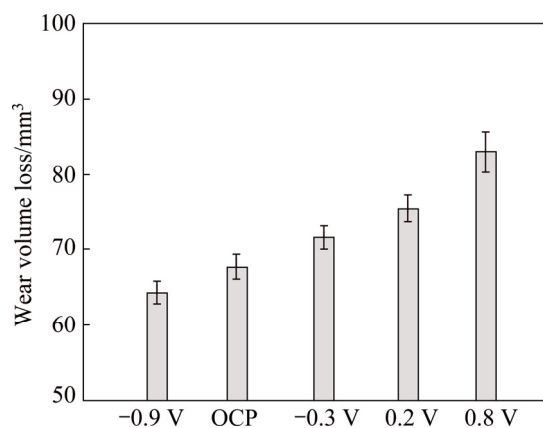


Fig. 6 Wear volume loss for TC4 alloy under different electrochemical conditions

3.3 Corrosion–wear synergy

Except common phenomena of cathodic change of OCP, increase of corrosion by wear and accelerated wear during corrosion–wear, the synergy effect between corrosion and wear especially under different electrochemical states should be discussed. Wear loss at -0.9 V can be regarded as the result of pure mechanical wear. In the existence of corrosion obtained from Fig. 6, either OCP or anodic potential state, wear loss is

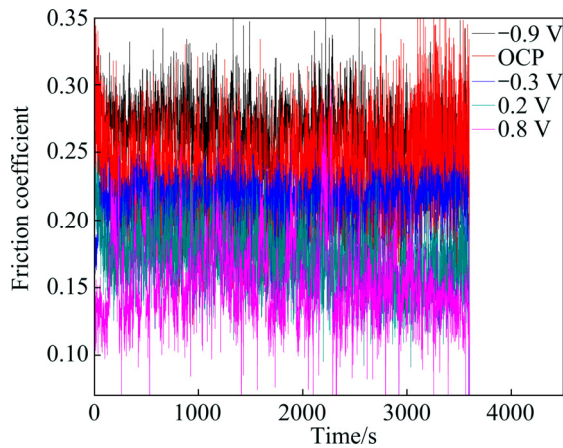


Fig. 7 Evolution of COF with time for TC4 alloy under different electrochemical conditions

accelerated. Current measurements and polarization curves (Figs. 3 and 5) also show the increase in corrosion rate. There is clear synergy between corrosion and wear, leading to corrosion-induced-wear and wear-induced-corrosion. Efforts have been made by many researchers to quantify such synergistic effect by the following general approach [6,21,26,27]. Wear loss can be explained:

$$K_{wc} = K_w + K_c \quad (2)$$

where K_{wc} is total wear loss, K_w is metal loss caused by wear, and K_c is material loss caused by corrosion. There, K_w can be divided into K_{w0} and ΔK_w :

$$K_w = K_{w0} + \Delta K_w \quad (3)$$

where K_{w0} is pure wear loss in the absence of corrosion, ΔK_w is wear loss owing to effect of corrosion on wear. And K_c can be divided into K_{c0} and ΔK_c :

$$K_c = K_{c0} + \Delta K_c \quad (4)$$

where K_{c0} is material loss caused by corrosion in the absence of wear, ΔK_c is material loss owing to effect of wear on corrosion, hence, total material loss caused by corrosion–wear can be expressed as follows:

$$K_{wc} = K_{w0} + \Delta K_w + K_{c0} + \Delta K_c \quad (5)$$

The corrosion loss from electrochemical process K_c is given by the Faraday's equation as

$$K_c = Q / (ZF) \quad (6)$$

$$K_c = Mit / (ZF) \quad (7)$$

where Q is the charge passed, Z is the number of electrons involved in corrosion process, F is the Faraday's constant (96500 C/mol), M is the relative atomic mass and can be calculated by considering the atomic fraction of components, I is the corrosion current and t is the corrosion time. As corrosion current cannot be directly measured under OCP, current value is taken as corrosion current calculated from polarisation curves shown in Fig. 3 by standard Tafel procedure. Current value under anodic potential conditions can be obtained by averaging the registered current in Fig. 5.

Results of various contributions to wear loss of TC4 alloy during corrosion–wear are given in Table 1. It can be obviously seen that pure corrosion without wear contributes insignificantly to total material loss, which indicates that the contribution of the term K_{c0} to total material loss can be negligible. This shows that at OCP and anodic potentials, mechanical wear contributes to 92.6%–96.7% of total material loss and only 3.3%–7.4% increment in metal loss is caused by corrosion–wear synergism. The contribution of mechanical wear loss to total material loss (K_w/K_{wc}) decreases slightly with the increase of potential. Overall, mechanical wear is dominated factor for TC4 alloy during corrosion–wear under this experimental condition.

The contribution of ΔK_c and ΔK_w to material loss of TC4 alloy should be discussed. When applied potential is increased to 0.8 V, wear-induced-corrosion and corrosion-induced-wear play dominant roles in the increment of metal loss. Figure 8 shows the fraction of ΔK_c , ΔK_w and K_{w0} to total material loss. Relative contribution of pure mechanical wear (K_{w0}) to total volume loss obviously decreases with the increase of potential from OCP to 0.8 V. Although electrochemical dissolution of TC4 alloy is significantly promoted and corrosion is increased by three hundreds of times by wear, the ratio of wear-induced-corrosion ΔK_c is not very high. Actually, it is 3.32% under OCP condition, and continuously increases to 7.83% at 0.9 V. Importantly, contribution of wear-induced-corrosion and corrosion-induced-wear becomes dominant especially at high potential.

Figure 9 shows the typical micrographs taken from wear tracks for TC4 alloy. It can be seen that the alloy

Table 1 Various component contribution to total volume loss

Potential	K_{wc}/mm^3	K_w/mm^3	K_c/mm^3	K_{w0}/mm^3	K_{c0}/mm^3	$\Delta K_w/\text{mm}^3$	$\Delta K_c/\text{mm}^3$	K_w/K_{wc}
OCP	68.73	66.45	2.28	64.12	0.0002	2.33	2.28	0.967
-0.3 V	71.54	68.4	3.14	64.12	0.0006	4.28	3.14	0.956
0.2 V	75.41	70.92	4.39	64.12	0.0011	6.8	4.39	0.941
0.8 V	82.92	76.8	6.12	64.12	0.0017	12.68	6.12	0.926

exhibits different failure mechanisms at different electrochemical states. Worn surfaces at -0.9 V are characterized by mainly severe deformation regions interrupted by furrows parallel to the sliding direction as shown in Fig. 9(a). The driving force for dissolution is negligible and deterioration is mainly through mechanical wear. Applied anodic potential can obviously affect the wear mechanism and surface morphologies. At OCP and -0.3 V, many wear debris can be observed in Figs. 9(b) and (c). Wear debris becomes large at 0.2 V and 0.8 V as shown in Figs. 9(d) and (e), exhibiting many cracks and micro-cracks in wear track. Failure

mechanism of passive film at anodic potential may be predicted. The deterioration process can be divided into three steps: 1) The oxide film formed in worn surface is divided into many big fragments and large cracks of passive film forms; 2) Micro-cracks form in the fragments and split into smaller parts, which cause local-fragmentation due to uneven distribution of contact stress; 3) Micro-fragments are removed due to friction and seawater impact, and then fresh oxide film forms. The continuous process of remove–repair in passive film results in large corrosion, leading to apparent wear-induced-corrosion. Corrosion-induced-wear can be

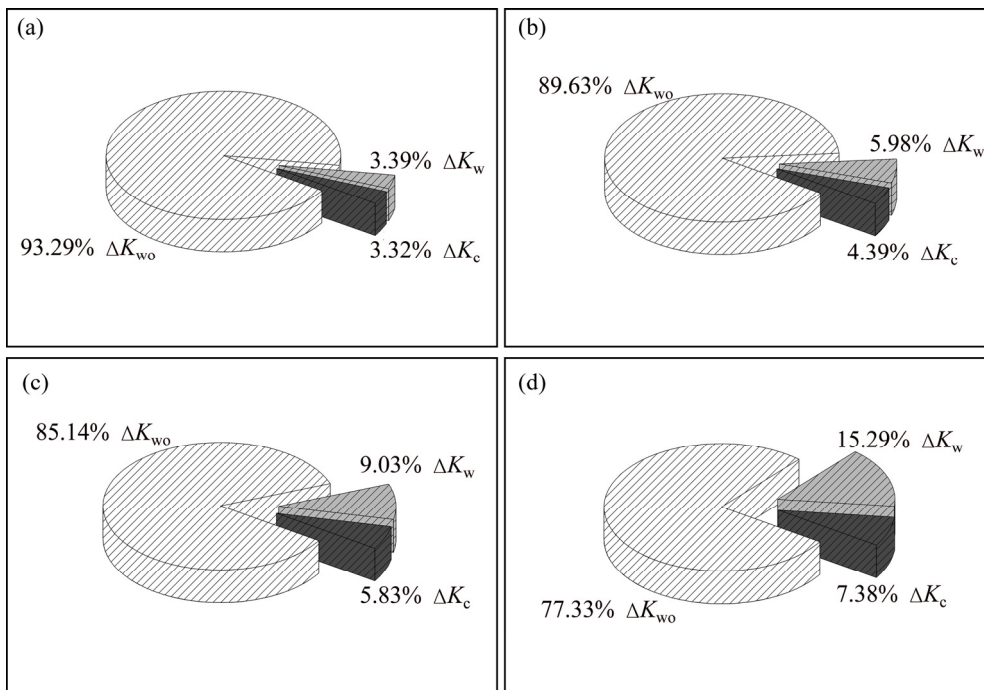


Fig. 8 Fraction of ΔK_c , ΔK_w and K_{w0} to total material loss for TC4 alloy: (a) OCP; (b) -0.3 V; (c) 0.2 V; (d) 0.8 V

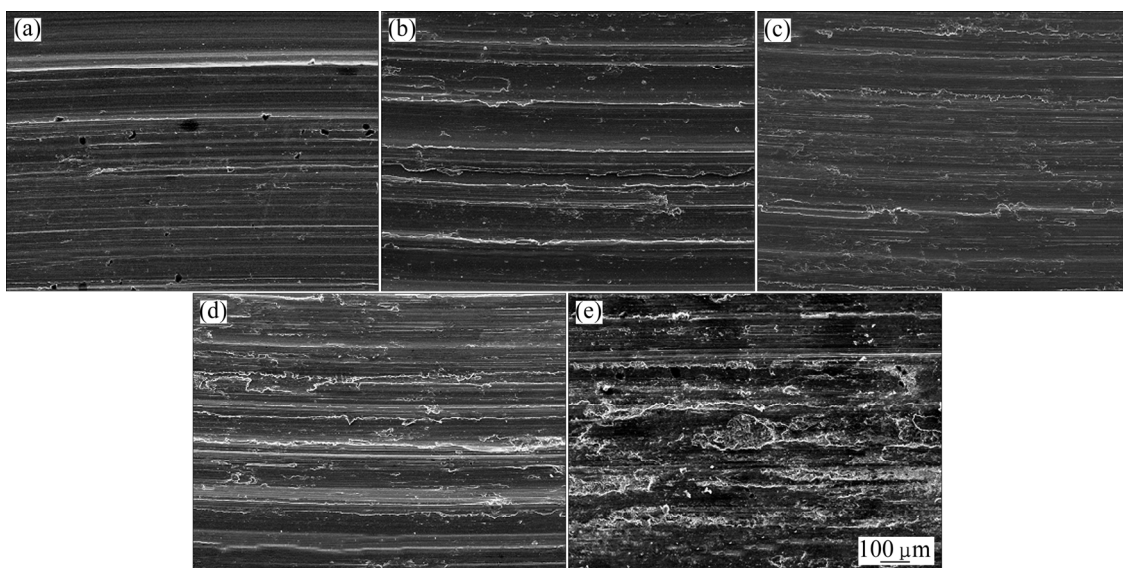


Fig. 9 Typical micrographs for TC4 alloy taken from wear tracks formed at different potentials: (a) -0.9 V; (b) OCP; (c) -0.3 V; (d) 0.2 V; (e) 0.8 V

understood through the failure mechanism of passive film. The form-fragment-remove-repair process of passive film becomes significant deterioration mechanism at high potential. Quick repair of destroyed passive film accelerates metal failure, resulting in dominant corrosion-induced-wear of TC4 alloy. Moreover, breakdown and remove of passive film reduce real area of contact for subsequent contact cycles, thus leading to higher contact stress and then higher wear rates also [26].

4 Conclusions

1) The cathodic shift of OCP due to sliding wear is confirmed and corrosion current density is increased by three orders of magnitude in anodic region.

2) Total corrosion–wear material loss increases obviously with increasing potential. There is a synergy between wear and corrosion. High potential results in low COF and high corrosion rate.

3) The relative contribution of pure mechanical wear to total material loss decreases obviously with the increase of potential from OCP to 0.9 V during corrosion–wear. The contributions of wear-induced-corrosion and corrosion-induced-wear are significant especially at higher potentials.

References

- [1] CHEN Jun, YAN Feng-yuan. Tribocorrosion behaviors of Ti–6Al–4V and Monel K500 alloys sliding against 316 stainless steel in artificial seawater [J]. Transactions of Nonferrous Metals Society of China 2012, 22(6): 1356–1365.
- [2] DING Hong-yan, DAI Zhen-dong, ZHOU Fei, ZHOU Guang-hong. Sliding friction and wear behavior of TC11 in aqueous condition [J]. Wear, 2007, 263(1–6): 117–124.
- [3] CHEN Jun, WANG Jian-zhang, YAN Feng-yuan, ZHANG Qing, LI Quan-an. Corrosion wear synergistic behavior of Hastelloy C276 alloy in artificial seawater [J]. Transactions of Nonferrous Metals Society of China 2015, 25(2): 661–668.
- [4] HIROMOTO S, MISCHLER S. The influence of proteins on the fretting–corrosion behaviour of a Ti6Al4V alloy [J]. Wear, 2006, 261(9): 1002–1011.
- [5] SERRE I, PRADEILLES-DUVAL R M, CELATI N. Tribological and corrosion experiments of graphite ring against Ti–6Al–4V disk: Influence of electrochemical and mechanical parameters [J]. Wear, 2006, 260(9–10): 1129–1135.
- [6] STACK M M, RODLING J, MATHEW M T, JAWAN H, HUANG W, PARK G, HODGE C. Micro-abrasion-corrosion of a Co–Cr/UHMWPE couple in Ringer’s solution: An approach to construction of mechanism and synergism maps for application to bio-implants [J]. Wear, 2010, 269(5–6): 376–382.
- [7] CHEN Jun, YAN Feng-yuan. Corrosive wear performance of Monel K500 alloy in artificial seawater [J]. Tribology Transactions, 2013, 56(5): 848–856.
- [8] ESPALLARGAS N, JOHNSEN R, TORRES C, MU OZ A I. A new experimental technique for quantifying the galvanic coupling effects on stainless steel during tribocorrosion under equilibrium conditions [J]. Wear, 2013, 307(1–2): 190–197.
- [9] LIU Jia, WANG Xue. Tribocorrosion behavior of DLC-coated CoCrMo alloy in simulated biological environment [J]. Vacuum, 2013, 92(6): 39–43.
- [10] MISCHLER S, MU OZ A I. Wear of CoCrMo alloys used in metal-on-metal hip joints: A tribocorrosion appraisal [J]. Wear, 2013, 297(1–2): 1081–1094.
- [11] BOESE E, ROTHIG J, GARZ I, SCHMIDTCHEN H. Tribocorrosion of stainless steels [J]. Materials and Corrosion-Werkstoffe Und Korrosion, 1998, 49(2): 98–107.
- [12] WATSON S W, FRIEDERSDORF F J, MADSEN B W, CRAMER S D. Methods of measuring wear corrosion synergism [J]. Wear, 1995, 181: 476–484.
- [13] MATHEW M T, ARIZA E, ROCHA L A, VAZ F, FERNANDES A C, STACK M M. Tribocorrosion behaviour of TiC_xO_y thin films in bio-fluids [J]. Electrochimica Acta, 2010, 56(2): 929–937.
- [14] MATHEW M T, NAGELLI C, POURZAL R, FISCHER A, LAURENT M P, JACOBS J J, WIMMER M A. Tribolayer formation in a metal-on-metal (MoM) hip joint: An electrochemical investigation [J]. Journal of the Mechanical Behavior of Biomedical Materials, 2014, 29: 199–212.
- [15] HENRY P, TAKADOUM J, BERCOT P. Tribocorrosion of 316L stainless steel and TA6V4 alloy in H₂SO₄ media [J]. Corrosion Science, 2009, 51(6): 1308–1314.
- [16] HENRY P, TAKADOUM J, BERCOT P. Depassivation of some metals by sliding friction [J]. Corrosion Science, 2011, 53(1): 320–328.
- [17] BARRIL S, MISCHLER S, LANDOLT D. Electrochemical effects on the fretting corrosion behaviour of Ti6Al4V in 0.9% sodium chloride solution [J]. Wear, 2005, 259(1–6): 282–291.
- [18] PRIYA R, MALLIKA C, MUDALI U K. Wear and tribocorrosion behaviour of 304L SS, Zr-702, Zircaloy-4 and Ti-grade2 [J]. Wear, 2014, 310(1–2): 90–100.
- [19] TEKIN K C, MALAYOGLU U. Assessing the tribocorrosion performance of three different nickel-based superalloys [J]. Tribology Letters, 2010, 37(3): 563–572.
- [20] SUN Y, RANA V. Tribocorrosion behaviour of AISI 304 stainless steel in 0.5 M NaCl solution [J]. Materials Chemistry and Physics, 2011, 129(1–2): 138–147.
- [21] IWABUCHI A, LEE J W, UCHIDATE M. Synergistic effect of fretting wear and sliding wear of Co-alloy and Ti-alloy in Hanks’ solution [J]. Wear, 2007, 263(1–6): 492–500.
- [22] PONTTHIAUX P, WENGER F, DREES D, CELIS J P. Electrochemical techniques for studying tribocorrosion processes [J]. Wear, 2004, 256(5): 459–468.
- [23] DIOMIDIS N, CELIS J P, PONTTHIAUX P, WENGER F. Tribocorrosion of stainless steel in sulfuric acid: Identification of corrosion-wear components and effect of contact area [J]. Wear, 2010, 269(1–2): 93–103.
- [24] SALASI M, STACHOWIAK G B, STACHOWIAK G W. New experimental rig to investigate abrasive-corrosive characteristics of metals in aqueous media [J]. Tribology Letters, 2010, 40(1): 71–84.
- [25] MISCHLER S, SPIEGEL A, STEMPEL M, LANDOLT D. Influence of passivity on the tribocorrosion of carbon steel in aqueous solutions [J]. Wear, 2001, 251: 1295–1307.
- [26] JIANG J, STACK M M, NEVILLE A. Modelling the tribo-corrosion interaction in aqueous sliding conditions [J]. Tribology International, 2002, 35(10): 669–679.
- [27] MISCHLER S. Triboelectrochemical techniques and interpretation methods in tribocorrosion: A comparative evaluation [J]. Tribology International, 2008, 41(7): 573–583.

模拟海水环境中电化学状态对 TC4 钛合金 腐蚀磨损行为的影响

陈君^{1,2,3}, 张清^{1,3}

1. 河南科技大学 材料科学与工程学院, 洛阳 471023;
2. 中国科学院 兰州化学物理研究所 固体润滑国家重点实验室, 兰州 730000;
3. 有色金属共性技术 河南省协同创新中心, 洛阳 471023

摘 要: 采用摩擦失重法、电化学测试以及扫描电子显微镜等技术研究 TC4 钛合金在模拟海水环境中的腐蚀和腐蚀磨损行为, 分析电化学状态对 TC4 钛合金钝化行为、钝化膜失效机制及腐蚀磨损协同作用的影响。结果表明, 摩擦过程中 TC4 钛合金的开路电位明显负移, 而且该合金的腐蚀电流密度相比静态腐蚀时提高了 3 个数量级。合金的腐蚀磨损失重随着电位的升高明显增大, 磨蚀与磨损之间存在明显的协同作用, 高电位时的腐蚀速度较大但是摩擦因数较低。电位在 OCP 和 0.9 V 之间变化时, 纯机械磨损量在总腐蚀磨损量中的比重随着电位的升高逐渐降低, 而磨损对腐蚀的促进量和腐蚀对磨损的促进量在总腐蚀磨损量中的比重在高电位时尤其显著。

关键词: TC4 合金; 腐蚀磨损; 电化学状态; 协同作用

(Edited by Xiang-qun LI)